MULTI-RESOLUTION SEISMIC TOMOGRAPHY BASED ON A RECURSIVE TESSELLATION HIERARCHY

Nathan A. Simmons, Stephen C. Myers, and Abelardo Ramirez

Lawrence Livermore National Laboratory

Sponsored by the National Nuclear Security Administration

Award No. DE-AC52-07NA27344/LL09-3Dseismic-NDD02

ABSTRACT

A 3-D global tomographic model that reconstructs velocity structure at multiple scales and incorporates laterally variable seismic discontinuities is currently being developed. The model parameterization is node based, with nodes being placed along vertices defined by triangular tessellations of a spheroidal surface. The triangular tessellation framework is hierarchical. Starting with a tetrahexahedron representing the whole globe (1st level of the hierarchy, 24 faces), we divide each triangle of the tessellation into daughter triangles. The collection of all daughter triangles composes the 2nd level of the tessellation hierarchy, and further recursion produces an arbitrary number of tessellation levels and arbitrarily fine node spacing. We have developed an inversion procedure that takes advantage of the recursive properties of the tessellation hierarchies by progressively solving for shorter wavelength heterogeneities. In this procedure, we first perform the tomographic inversion, using a tessellation level with coarse node spacing. We find that a coarse node spacing of approximately 8° is adequate to capture bulk regional properties. We then conduct the tomographic inversion on a 4° tessellation level using the residuals and inversion results from the 8° run. In practice we find that the progressive tomography approach is robust, providing an intrinsic regularization for inversion stability, and avoids the issue of predefining resolution levels. Further, determining average regional properties with coarser tessellation levels enables long-wavelength heterogeneities to account for sparsely sampled regions (or regions of the mantle where longer wavelength patterns of heterogeneity suffice) while allowing shorter length-scale heterogeneities to emerge where necessary.

We demonstrate the inversion approach with a set of synthetic test cases that mimic the complex nature of data arrangements (mixed-determined inversion) common to most tomographic problems. We also apply the progressive inversion approach with *Pn* waves traveling within the Middle East region and compare the results to simple tomographic inversions. As expected from synthetic testing, the progressive approach results in detailed structure where there is high data density and broader regional anomalies where seismic information is sparse. The ultimate goal is to use these methods to produce a seamless, multi-resolution global tomographic model with local model resolution determined by the constraints afforded by available data. We envisage this new technique as the general approach to be employed for future multi-resolution model development with complex arrangements of regional and teleseismic information.

OBJECTIVES

The objective of this 3-year project is to create a seamless, 3-D tomographic model that reconstructs seismic heterogeneities at regional and global scales to enhance seismic event location capabilities through more-accurate travel time predictions. To achieve this overall objective, multiple sub-objectives must be achieved, including the following:

1. The development of a modeling framework that efficiently allows variations in continuous media, as well as discontinuities at geologic boundaries;
2. Fully 3-D ray tracing algorithms that communicate with such a framework to predict accurate travel times and define path sensitivities to the 3-D model space; and
3. A stable tomographic inversion technique that is suited to solve for structures at fine and broad scales simultaneously given the available seismic information and the variations of heterogeneity wavelengths often observed in Earth's crust and mantle.

Because variants of Objectives 1–2 have been outlined in previous MRR reports, the primary focus of the current report regards the development of a tomographic inversion technique (Objective 3) tailored to reconstruct 3-D seismic heterogeneity on multiple resolution scales. The technique takes advantage of the recursive nature of a tessellation-based model framework and eliminates the requirement of traditional regularization operators and/or pre-defining variable model parameter densities.

RESEARCH ACCOMPLISHED

As part of the Ground-based Nuclear Explosion Monitoring (GNEM) R&D program, we are developing a singular, global 3-D seismic model for the primary purpose of enhancing seismic event location capabilities. Our goal is to produce a model within a framework suitable for accurate and efficient computation of travel times without the strict requirement for station-phase-specific lookup tables and/or empirical corrections. We have made significant advances towards achieving this goal by focusing on the development of advanced tomographic inversion techniques required to generate accurate representations of Earth structure with complex arrangements of seismic information.

Model Framework and Starting Model Design

Our model representation is based upon a triangular tessellation procedure whereby the triangular facets of an initial object (in our case, a tetrahexahedron) are recursively broken down into smaller sub-triangles and projected onto a unit sphere (Figure 1). This general procedure has been adapted by multiple scientific disciplines including the representation of seismic models of the Earth (e.g. Wang & Dahlen 1995; Ishii & Dziewonski 2002; Ballard et al. 2008a; Myers et al. 2009). Each subdivision of a triangular facet ("parent") produces 4 triangular facets ("daughters"), thereby increasing the number of points and the resolution upon each recursion step. We refer to all sequentially produced objects as "Levels," starting with the initial object (Level 1; Figure 1a) up to Level *N*. In our case, model nodes are placed at any arbitrary distance (radii) along the vertices of the triangles, allowing for the representation of a spheroidal Earth with undulating layers (Figure 2b). For instance, Moho depth is independently defined along each geocentric vector, and continuous Moho depth within each tessellation triangle is determined by interpolating the set of nodes or "nodesets" that define each triangle.

The major benefit of the tessellation-based model design is the efficiency of referencing a complex model at any arbitrary location through a process called hierarchical triangulation (Figure 1). The 1st-level triangle containing the point of interest is found first, using basis vector arithmetic. Then only daughters of that 1st-level triangle are searched until the 2nd-level triangle containing the point is found. This hierarchical search is repeated to the desired tessellation level. Indexing parent-daughter triangle relationships from one tessellation level to the next allows for rapid identification of the vertices surrounding the point of interest at each successive tessellation involving testing a maximum of $24+4(N-1)$ triangles, where N represents the final level. For example, if we were interested in finding the triangle that encompasses a point at Level 7 (98,304 triangles; ~1° vertex spacing), we would need only to search a maximum of $24+4(7-1)=48$ triangles.

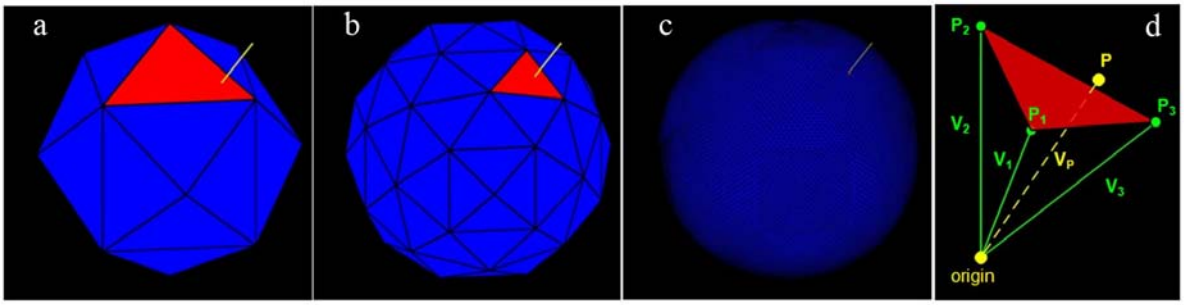

Figure 1. Tessellation-based model representation. The 24 triangular facets of a tetrahexahedron (a, Level 1) are recursively subdivided into 4 small triangular facets to produce a total of 96 faces (b, Level 2). The process is repeated to generate 24,576 faces with 12,290 vertices (c, Level 6). By defining a vector (yellow line) from the origin to a point *P* in space, the point can be quickly associated with a particular triangular facet at any tessellation level (red triangles) defined by vectors (V_1, V_2, V_3) through a process called hierarchical triangulation.

After identifying the triangle, we then compute barycentric (or areal) coordinates for each of the three points defining the triangle. These coordinate values are equivalent to weights placed at each node needed to physically balance the triangle at the arbitrary point *P* (Figure 2a). These coordinates serve as lateral interpolation weights for any model properties, including seismic velocities, velocity gradients, and nodeset radii. The laterally interpolated values for each bounding nodeset are then linearly interpolated in the radial direction along the point-of-interest vector (POI, Figure 2b), and simple linear interpolation determines the model property at the POI.

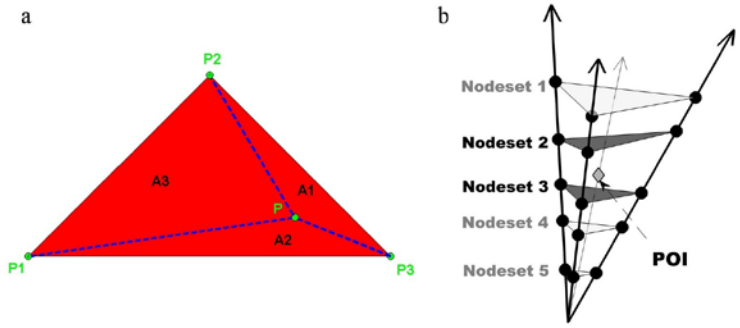

Figure 2. Schematic representation of the interpolation procedure to attain model properties at any arbitrary point. (a) Barycentric (or areal) coordinates serve as interpolation weights. Physically, these values are the masses required at each point defining the triangle to balance it about point *P*. Geometrically, these values are equivalent to the ratio of the opposite areas (*A1*, *A2*, *A3*) of the triangle normalized by the total area. For example, the barycentric weight at *P3* is *A3*/(*A1*+*A2*+*A3*). (b) The nodesets surrounding the POI are identified, and the model properties are computed at the intersection of the POI vector with the nodeset plane. Simple linear interpolation in the radial direction is then used to compute the model property at the POI.

We chose to build a starting global 3-D model within this framework suitable for reasonable 1st-order estimation of seismic ray paths, travel times, and testing purposes. The model integrates the components of the regional travel time model RSTT from Myers et al. (2009) and the global 3-D P-wave velocity model MIT-P08 from Li et al. (2008). The properties/components of the designed model include the following:

1) Spheroid (based on the GRS80 ellipsoid)
2) Tetrahexahedron build at Level 7 (~1° node spacing) down to 310 km below the spheroid
3) Tetrahexahedron build at Level 6 (~2° node spacing) below 310 km

4) Water, ice, sediment, and crustal layers from the RSTT model (7 discontinuous layers)
5) *Pn* and shallow upper-mantle velocities computed from the RSTT model (down to 120 km)
6) Averaged P-wave velocities from the RSTT and MIT-P08 models at 120 km
7) Discontinuous upper-mantle transition zone layers
8) P-wave velocity from 120 km below the spheroid to the core-mantle boundary from MIT-P08.

This designed model has served as a testing ground for 3-D ray tracing algorithm design and a starting solution for the real test case described within the remainder of this report.

3-D Ray Tracing and Sensitivity Kernel Definitions

In order to accurately predict travel times and model space sensitivities in complex 3-D media, we have adapted a 3-D ray tracing procedure specifically tailored to communicate with the aforementioned model design. The general approach we have taken is based on the techniques originally conceived by Zhao et al. (1992) to model direct arrivals within a subduction zone and extended to teleseismic phases by Zhao and Lei (2004). The technique uses pseudo-bending in continuous media developed by Um and Thurber (1987) while simultaneously satisfying Snell's Law at discontinuous interfaces through an iterative process. One major shortcoming of this approach is the inability to find global minimum travel times and paths for complex regional phases such as *Pn*. We have therefore adapted the procedure to find such global minima (Figure 3).

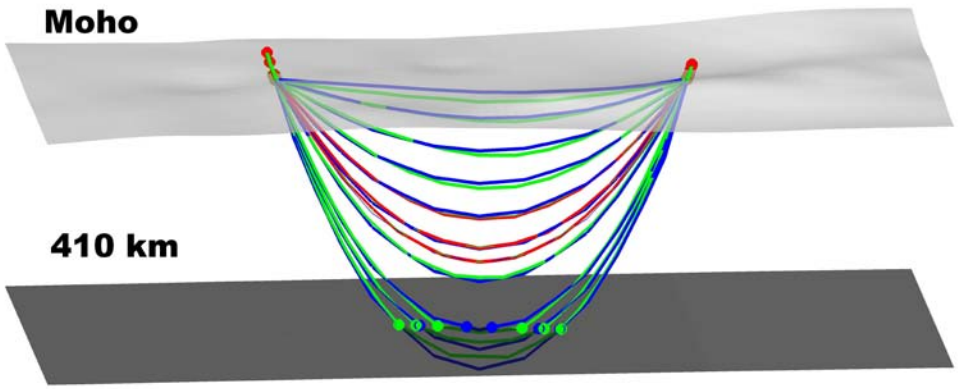

Figure 3. Example of a pseudo-bending/interface 3-D ray tracing approach for an 18° path. Initial path estimates (blue) are based on perturbations of the expected path for a 1-D Earth and a logical set of rules that define the possible paths for a given event-station pair. Two pseudo-bending iterations combined with enforced interface boundary conditions (Zhao et al. 1992) are performed to yield refined paths (green). All refined paths yielding a travel time within some tolerance of the minimum travel time provided by the set are further refined. Those paths yielding a travel time very near the minimum are kept (red) and form the basis of the sensitivity kernels used in the inversions. Note: the circles represent interface piercing points at all discontinuous boundaries along the paths. Only two such boundaries are shown (Moho and 410 km discontinuity).

In our approach, we initially create several crude ray path estimates based upon the 1-D ray path expectation. Each of the possible paths is iteratively perturbed within the 3-D media according to the pseudo-bending/interface technique (Zhao et al. 1992). Paths that are within some tolerance (we chose 1 second) of the minimum time are perturbed until convergence. The final possible paths are then defined as paths that generate the minimum time within a smaller time tolerance (we chose 0.2 seconds). These paths (Figure 3; red) form the basis for the sensitive kernel for a specific event/station pair and our inverse system of equations. A similar adaptation has recently been developed by Ballard et al. (2008b), in which the computational process was designed within a distributed parallel environment. Ballard et al. (2008b) demonstrated the ability to dramatically improve the efficiency of the technique,

thus providing support for the implementation of the approach for routine seismic event location. Moreover, our comparison of travel times computed through a finite difference technique has shown significant travel time disagreements with the more accurate 3-D ray tracing procedure that accounts for detailed undulations of discontinuous boundaries.

Inversion Technique and Synthetic Example

Traditional tomographic inversion approaches involve predefining a model space with a single set of parameters (nodes or constant-property blocks) that represent some part of the Earth. For a given set of seismic ray paths, sensitivity kernels are designed to represent travel time sensitivity to a number of these predefined model parameters. These sensitivities are collected into a matrix (**A**), and the residual travel times relative to some starting velocity model represent the data (***b***). Together, they form a forward system of equations **Ax=b**. In this linear system of equations, **x** is an unknown vector of slowness perturbations to be determined through an inversion routine. The inversion procedure is often unstable due to the mixed-determined nature of typical tomographic datasets. This requires some form of regularization such as damping (**D**) and/or smoothing (**S**) operators to stabilize the solution:

$$\begin{bmatrix} \mathbf{A} \\ w_d\mathbf{D} \\ w_s\mathbf{S} \end{bmatrix} \mathbf{x} = \begin{bmatrix} \mathbf{b} \\ \mathbf{0} \\ \mathbf{0} \end{bmatrix}$$

where w_d and w_s are damping and smoothing weights, respectively. For very ill-posed problems, determining the optimum weights is difficult and sometimes speculative. Mixing teleseismic and dense clusters of regional seismic information presents one such ill-posed problem in which we have an abundance of information in certain regions and a lack of information in other regions. Moreover, the standard tomographic technique requires the predefinition of a set of static model parameters, thereby defining the resolution level of the outcome model *a priori*.

The "progressive" inversion technique circumvents the need for predefining resolution scale and significantly reduces the need for regularization. The basic idea behind the approach is to solve for structure initially at lower resolutions before proceeding to finer detail. In doing so, long-wavelength regional trends are resolved first, which may be accomplished in regions with dense or sparse data coverage. Upon each step up in resolution, finer detail structures emerge from the regional trends only where it is necessary to explain the given set of observations. Therefore, data drive the resulting variable resolution scales rather than a predefinition of variable node densities and regularization operators. The technique is best described by the algorithm

$$\begin{aligned} &\mathbf{x}_1 = \mathbf{A}_1^{-1}\mathbf{b}_1 \\ &for\ i = 2 \ldots n \\ &\qquad \mathbf{b}_i = \mathbf{b}_{i-1} - \mathbf{A}_{i-1}\mathbf{x}_{i-1} \\ &\qquad \mathbf{x}_i = \mathbf{x}_{i-1} + \mathbf{A}_i^{-1}\mathbf{b}_i \\ &end \end{aligned}$$

In this algorithm, the subscripts denote the recursion level (or resolution level). The superscript "-1" refers to matrix inversion and the variables **A**, **x**, and **b** are the sensitivity kernels, slowness perturbation models, and residual data vectors, respectively. After each iteration, the travel time signals produced by the previous lower-resolution model is removed and the previous model is effectively used as the starting solution in the next stage. In the case of a tessellation-based model, $\mathbf{A}_1$ would correspond to sensitivity kernels defined on the starting object (i.e., the 1st-level

tessellation; in our case a tetrahexahedron), and $\mathbf{A}_2$ would correspond to sensitivities built upon the nodes defined by the 2nd-level tessellation (see Figure 1).

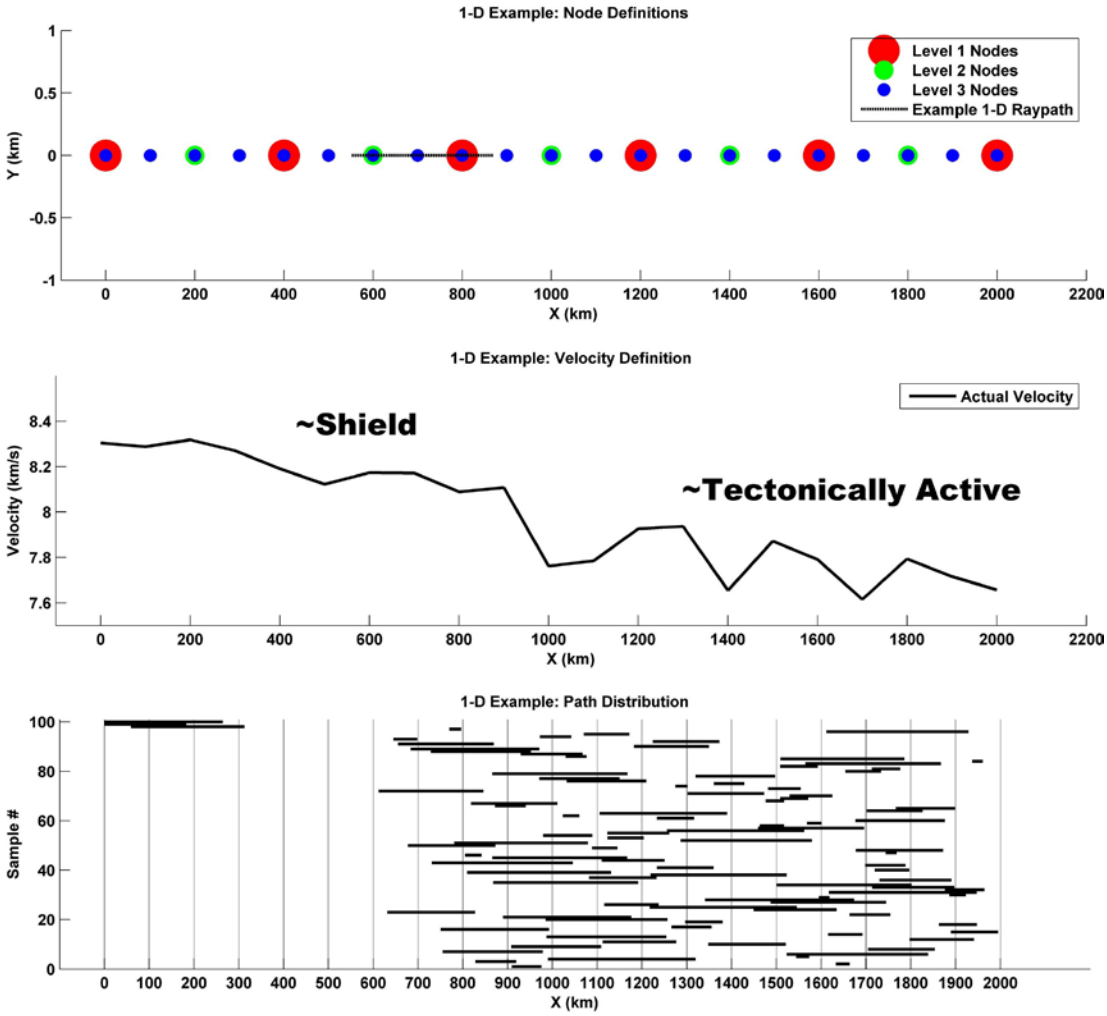

Figure 4. Synthetic inversion test case along a line with varying velocity. (Top) Node definitions at 3 recursion levels. (Middle) Node velocity definitions that are meant to simulate a high-velocity shield that is relatively homogeneous, and a lower-velocity tectonic region that is inhomogeneous. (Bottom) An example 1-D ray path distribution yielding a mixed determined set of linear equations. This arrangement of data is not uncommon to real tomographic cases in which few data may be available in an aseismic shield region and an abundance of data in a tectonic region.

To evaluate the behavior of this inversion technique, we devised a simple 1-D synthetic test case that mimics an ill-posed, mixed determined tomographic problem (Figure 4). For this synthetic test, we placed 6 equally spaced nodes along a line to represent the 1st recursion level (Figure 4, top). Points were then placed at the midpoints between the 1st level points. These points, along with the 1st level points, comprise of the 2nd recursion level. This recursion was repeated once again to give a total of 21 node points. For a single test, we then randomly generated 100 ray paths along the line of points while forcing a much larger number of paths to be to one end of the line to mimic a mixed-determined problem. Travel times were calculated on the basis of a known starting model, and a substantial amount of random noise (standard deviation of 0.5 seconds) was added to complete the setup of an ill-posed inversion problem. We randomly generated ray paths (and data) 100 times while regulating the system with a range of simple damping weights. For each realization of paths and noise, we inverted the resulting system of

equations using a simple inversion approach (directly inverted at the highest level) and the progressive inversion approach. It is concluded from these tests that the progressive inversion method is most capable of reproducing the known velocity model (Figure 5). In particular, the approach simultaneously resolves the long-wavelength regional trend, where the system is underdetermined, and the shorter-wavelength structures where there is sufficient data. With this synthetic test case design, it is difficult to accurately reproduce the known model with a simple inversion given the mixed determined nature of the problem and the realistic noise characteristics.

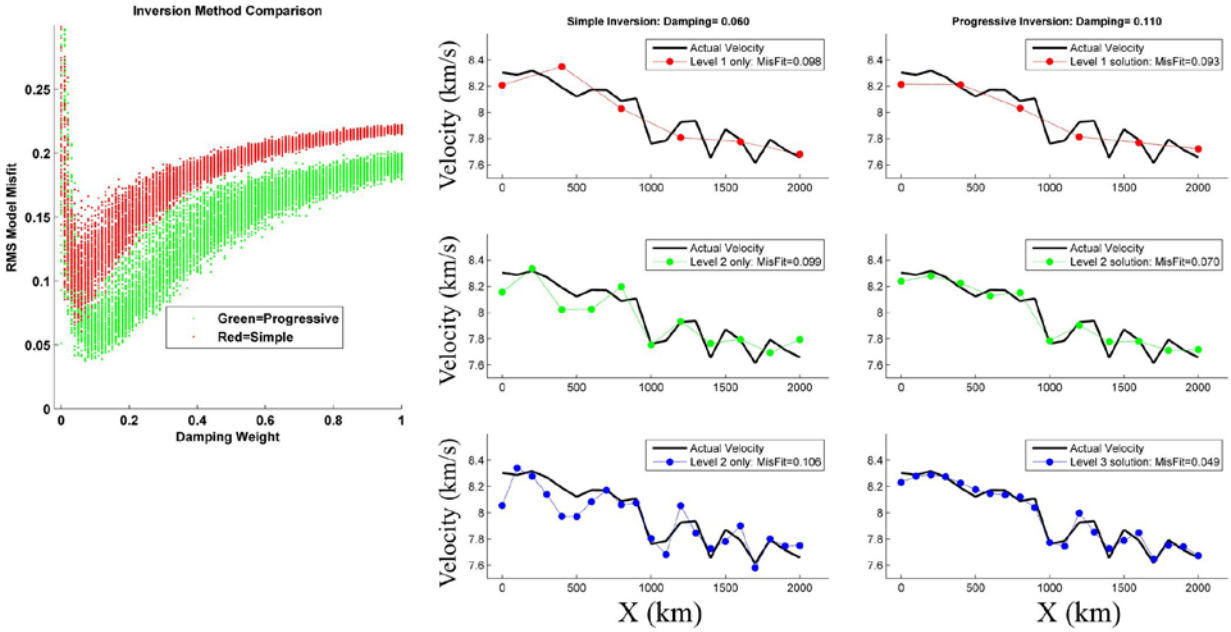

Figure 5. Comparison of simple and progressive inversion methods. (Left) RMS misfit to the known model for 10,100 data realizations and each inversion technique. The progressive inversion approach most often yields models most closely resembling the known solution. (Middle) A simple inversion solution for an arbitrary data realization with the optimum damping for that case. (Right) Progressive inversion solution for the same realization as the simple inversion case.

Application to Middle East *Pn* Data

The next phase in the evaluation of the progressive inversion technique is application to real data in a fully 3-D model space. We compiled *Pn* summary travel times from the Lawrence Livermore National Laboratory (LLNL) database for events occurring in the Middle East region and seismic stations located within 15° of the initial event locations (Figure 6). Event locations were revised through the probabilistic multiple event locater (BayesLoc) described in Myers et al. (2007, 2009), and the data were reduced to ~19,000 summary arrivals. Ray paths were computed using our 3-D ray tracing algorithms on the basis of the global 3-D model design discussed above. Because small variations in velocity can dramatically change the ray path, all 3-D ray paths that generated travel times within 0.2 seconds of the minimum path time for each event-station pair were used to construct the tomographic sensitivity kernel. This approach allows the whole tomographic dataset to help in the determination of the minimum-time ray. Sensitivity kernels were developed for nodes defined at tessellation Level 4 (~8° node spacing), Level 5 (~4° node spacing), Level 6 (~2° node spacing), and Level 7 (~1° node spacing).

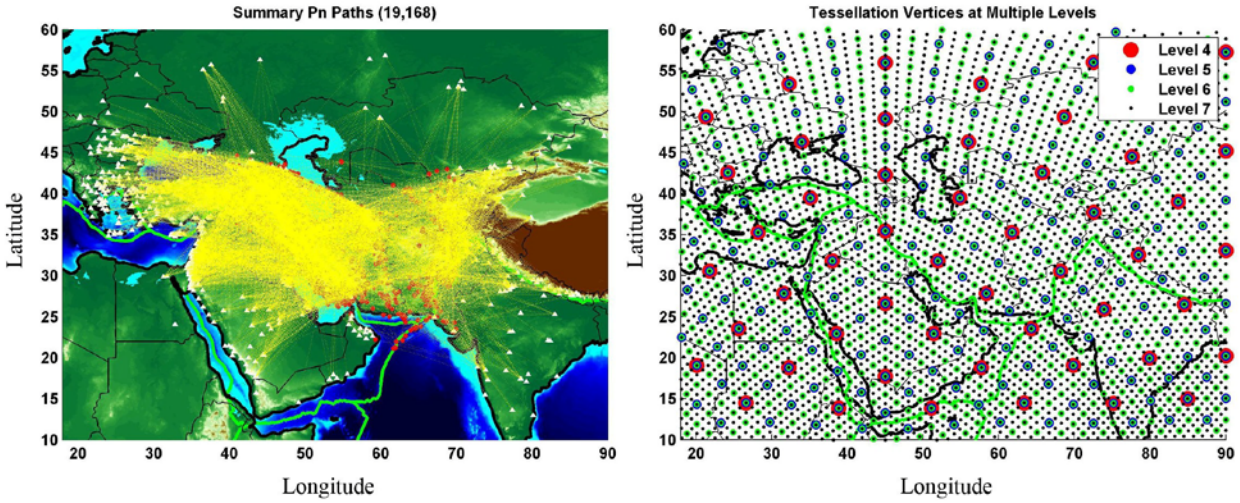

Figure 6. *Pn* paths and tessellation vertices in the Middle East region.

Tomographic inversions using the simple (direct inversion at the highest tessellation level) and progressive techniques were performed to image the shallow upper mantle beneath the Middle East and surrounding regions. Similar to the synthetic case, we performed the inversions with the iterative LSQR routine of Paige and Saunders (1982) considering a range of damping weights. It should be noted that smoothing constraints were not incorporated. Although the complex 3-D starting model was employed as the basis for computing the 3-D ray paths and sensitivity kernels, we chose to use an average model as the starting solution in order to best demonstrate the inversion procedure. Thus, we selected the average values within nodesets (such as the nodeset defining the *Pn* layer, etc.) as the values to perturb in 3-D.

The resulting *Pn* velocity structures and effects of damping weight are illustrated in Figure 7. At any given damping weight, the progressive inversion approach yields models that are more consistent with the data than is a simple inversion. There are multiple causes for this result, including the fact that the total number of LSQR iterations performed varies amongst the inversion techniques. More specifically, we performed 64 LSQR iterations at each progression. Therefore, the total number of iterations is 64*4 for the progressive approach, while 64*1 iterations were executed for the simple inversion. This evaluation is not entirely even; however, we find that increasing the number of total iterations for the simple inversion results in unreasonably rough models and marginal improvement to data fit.

The models selected for comparison (Figure 7) are very similar where there is an abundance of data (i.e., along the Zagros mountain chain). One of the major differences between the two solutions is the streaky behavior exhibited with the simple inversion where data are sparse and crossing ray paths are nonexistent (see Figure 6). On the other hand, the progressive approach produces long-wavelength structures in these regions and a smooth transition from these poorly sampled zones to the more detailed structures along the Zagros chain. This effect is consistent with our results from the synthetic 1-D case outlined in this report. Consequently, the progressive approach produces models that are multi-resolution without *a priori* declaration of node density variations. The approach also circumvents the requirement for smoothing constraints that would likely necessitate decisions regarding optimum smoothing levels and regional variations of smoothing kernels to achieve a similar result. In effect, the procedure allows the data rather than the modeler to drive the resolution level.

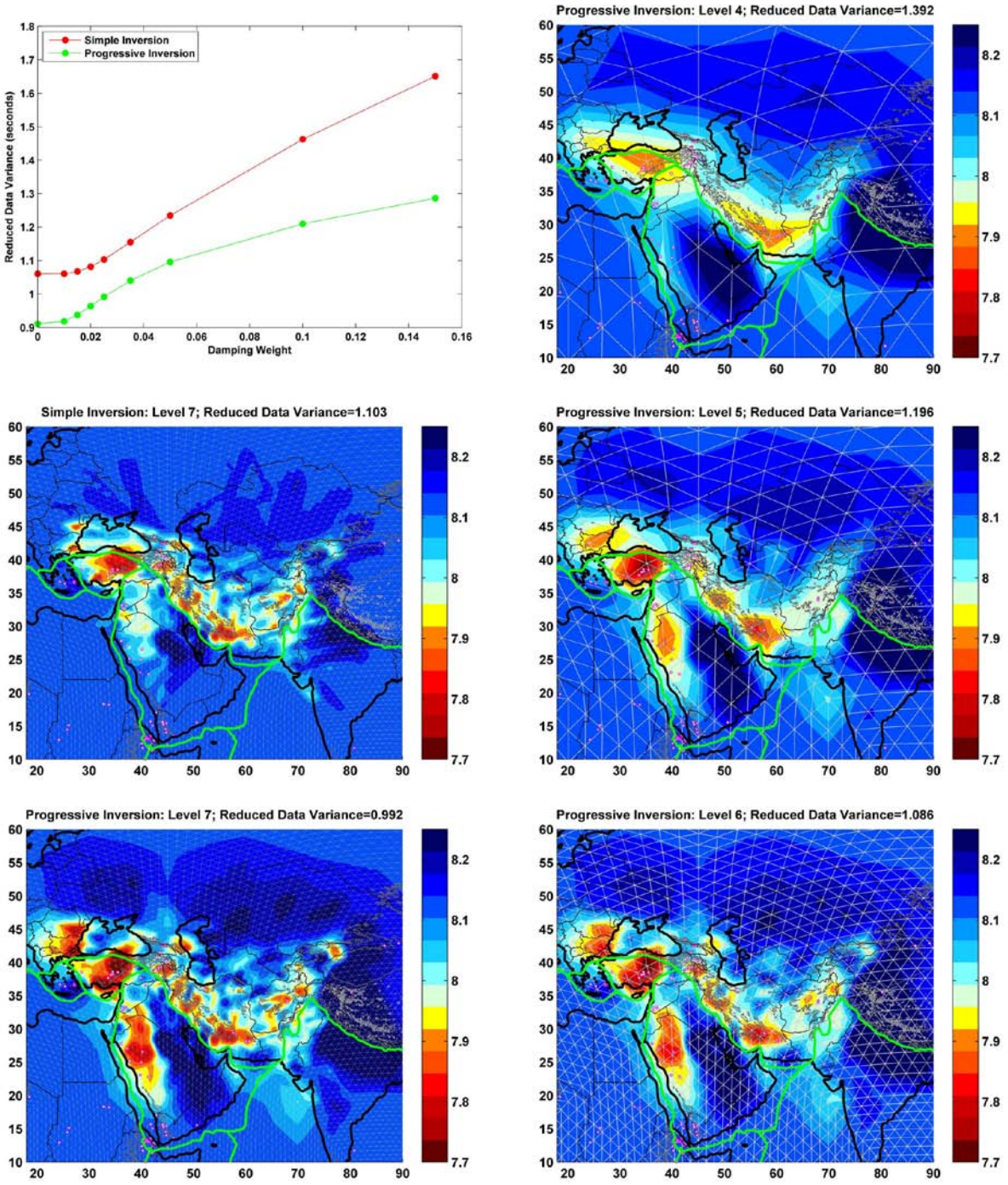

Figure 7. ***Pn*** **velocity structure in the Middle East and surrounding regions determined through a simple inversion and the progressive approach. (Left Column) Data misfit as a function of damping weight and solutions for each case with a damping weight of 0.025. The simple inversion exhibits streaks and spikes where data are limited, whereas the progressive inversion generates long-wavelength regional trends smoothly transitioning into zones with more-detailed information. (Right Column) The progressive inversion results at each stage of the progression.**

CONCLUSIONS AND RECOMMENDATIONS

The development of a self-consistent regional/global-scale 3-D model for the enhancement of event location capabilities requires advanced inversion techniques to adequately capture structure at multiple scales with complex configurations of seismic information. We developed an inversion approach based on the recursive nature of a tessellation model design that allows such models to be produced without pre-defining node densities or optimizing smoothing conditions. This approach is a viable technique for further development of global, multi-resolution 3-D seismic models.

REFERENCES

Ballard, S., J. Hipp, and C. Young (2008a). Robust, extensible representation of complex Earth models for use in seismological software systems, in *Proceedings of the 30th Monitoring Research Review: Ground-Based Nuclear Explosion Monitoring Technologies*, LA-UR-08-05261, Vol. 1, pp. 347–355.

Ballard, S., J. Hipp, C. Young, G. T. Barker, M. Chang (2008b). Implementation of a pseudo-bending seismic travel time calculator in a distributed parallel computing environment, in *Proceedings of the 30th Monitoring Research Review: Ground-Based Nuclear Explosion Monitoring Technologies*, LA-UR-08-05261, Vol. 1, pp. 338–346.

Ishii, M. and A. M. Dziewonski (2002). The innermost inner core of the Earth: Evidence for a change in anisotropic behavior at the radius of about 300 km, *PNAS* 99: 14026–14030.

Li, C., R. D. van der Hilst, E. R. Engdahl, and S. Burdick (2008). A new global model for P wave speed variations in Earth's mantle, *Geochem. Geophys. Geosystems* 9: 1–21.

Myers, S. C., G. Johannesson, and W. Hanley (2009). Incorporation of probabilistic seismic phase labels into a Bayesian multiple-event locator, *Geophys. J. Int*. 177: 193–204.

Myers, S. C., G. Johannesson, and W. Hanley, A Bayesian hierarchical method for multiple-event seismic location, *Geophys. J. Int*. 171: 1049–1063.

Paige, C. C. and M. A. Saunders (1982). LSQR: An algorithm for sparse linear equations and sparse least squares, *ACM Trans. Math. Soft*. 8: 43–71.

Um, J. and C. Thurber (1987). A fast algorithm for two-point seismic ray tracing, *Bull. Seis. Soc. America*, 77: 972–986.

Wang, Z. and F. A. Dahlen (1995). Spherical-spline paramterization of three-dimensional Earth, *Geophys. Res. Lett*. 22: 3099–3102.

Zhao, D., A. Hasegawa, and S. Horiuchi (1992). Tomographic imaging of P and S wave velocity structure beneath northeastern Japan, *J. Geophys. Res.* 97: B13, 19909–19928.

Zhao, D. and J. Lei (2004). Seismic ray path variations in a 3D global velocity model, *Phys. Earth. Planet. Int.* 141: 153–166.